

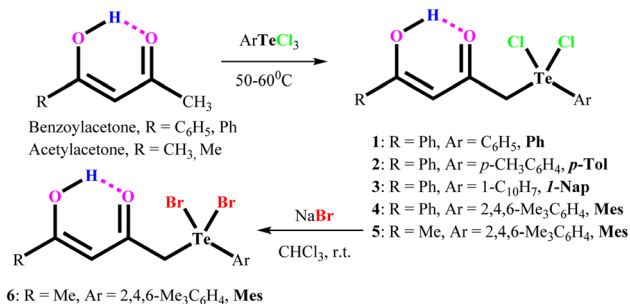
Chart 2 Reported organoselenium and organotellurium derivatives of acetylacetone.

atoms of acetylacetone are covalently bonded with Sb atoms in the trichloro(acetylacetonato)phenylantimony(v).²²

Similarly, methyl fragments bearing ketones can undergo electrophilic substitution reactions with aryltellurium trichlorides under mild conditions to obtain the aryl(acylmethyl) tellurium dichlorides Ar[RC(O)CH₂]₂TeCl₂ (Ar = phenyl, *p*-tolyl, *p*-anisyl, 1-naphthyl, mesityl; R = Me, *i*-Pr, *t*-Bu, mesityl).²³ In the present study, we create the carbonyl functionalized organotellurium(IV) derivatives, Ar[RC(OH)CHC(O)CH₂]₂TeCl₂ (1–5) [Ar = phenyl, (Ph); *p*-tolyl, (*p*-tol) 1-naphthyl, (1-Nap); and mesityl (Mes); R = methyl, phenyl] through the treatment of acetylacetone or benzoylacetone with aryltellurium trichlorides under mild conditions. In addition, Mes[CH₃C(OH)CHC(O)CH₂]₂TeBr₂ (6) are also prepared through the metathetical reaction of 5 with NaBr in chloroform at room temperature.

2 Result and discussion

Aryltellurium trichlorides react under mild conditions with acetylacetone/benzoylacetone to give proton responsive unsymmetrical diorganotellurium(IV) dichlorides, Ph[PhC(OH)CHC(O)CH₂]₂TeCl₂, (1); *p*-Tol[PhC(OH)CHC(O)CH₂]₂TeCl₂, (2); 1-Nap[PhC(OH)CHC(O)CH₂]₂TeCl₂, (3); Mes[PhC(OH)CHC(O)CH₂]₂TeCl₂, (4); and Mes[MeC(OH)CHC(O)CH₂]₂TeCl₂, (5) (Scheme 1).



Scheme 1 Development of carbonyl functionalized organotellurium(IV) derivatives.

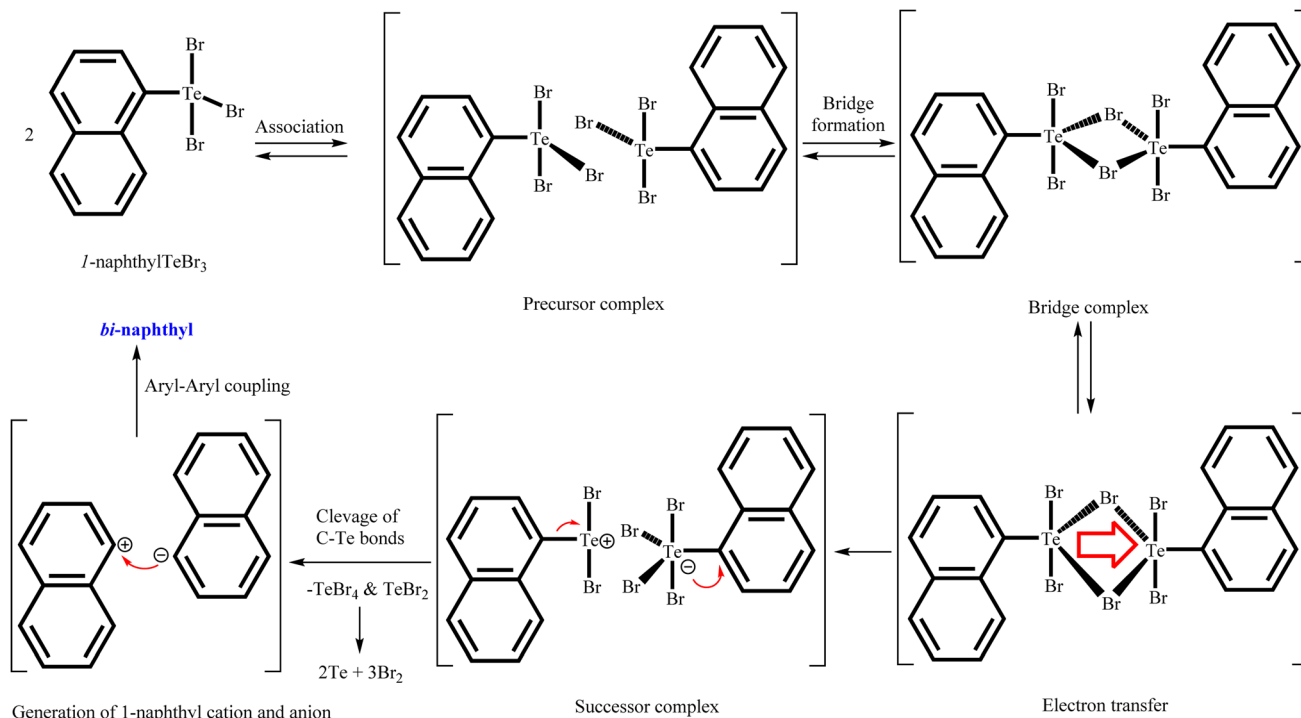
The aryltellurium trichlorides employed have two axial and one equatorial chlorine atoms along with the aryl fragment. Only the equatorial chlorine atom of the aryltellurium trichlorides participates in the reactions.²³ We can conclude that aryl fragment have more *trans* directing effect than the chlorine atoms in the aryltellurium trichlorides. However, the reaction of 1-naphthyltellurium triiodide with benzoylacetone did not take place, even at temperatures up to 60 °C. Similarly, decomposition takes place during reaction of 1-naphthyltellurium tribromide, affording the bi-naphthyl product through aryl–aryl coupling.

Plausible mechanism for aryl–aryl coupling are shown in Scheme 2. The first two steps are the formation of a precursor complex and the formation of bridged binuclear intermediate. Subsequently electron transfer through the bridging ligand to give the successor complex, followed by dissociation to 1-naphthyl cation, 1-naphthyl anion, TeBr₄ and TeBr₂. Finally, 1-naphthyl cation and anion undergo aryl–aryl coupling to give bi-naphthyl product. Simultaneously, during dissociation process also afforded two equivalent of elemental Te and three equivalent of elemental Br₂ through decomposition of *in situ* generated TeBr₄ and TeBr₂.

The dibromide Mes[PhC(OH)CHC(O)CH₂]₂TeBr₂, (6) can also be obtained with 95% yield from the corresponding dichlorides by metathesis with NaBr in chloroform at room temperature. Biphase (H₂O/CH₂Cl₂) reduction of dichlorides 1–5 with Na₂S₂O₅ affords respective labile tellurides, which decompose quickly even at room temperature into the more stable symmetric ditellurides, Ar₂Te₂. The filtrate showed the presence of parent ketone (¹H NMR).

All the proton responsive unsymmetrical diorganotellurium(IV) dihalides are crystalline solids that are soluble in common organic solvents. The ¹H and ¹³C{¹H} NMR spectra of the mesityltellurim(IV) derivatives are quite interesting. The restricted rotation of the mesityl fragment about the Te–C(mesityl) bond in 4, 5 and 6 is evidenced from their ¹H NMR spectra, which show separate signals for each of the *meta* ring protons and those of the two *ortho* methyl groups.^{23,24} All of the





Scheme 2 Plausible mechanism for aryl-aryl coupling.

corresponding $^{13}\text{C}\{^1\text{H}\}$ NMR spectra consist of separate signals for each of the six ring and the two *ortho* methyl carbon atoms. The ^1H chemical shifts for the CH₂, CH and OH protons of the ketone fragments in 1–6 show singlets at ~ 5 , ~ 6.22 and ~ 15.12 ppm respectively.

The ^{125}Te NMR of all the isolated diorganotellurium(IV) derivatives (1–6) show the presence of only one tellurium containing species in solution, as well as in the solid state. A single resonance signal suggests they are stable in solution state. The ^{125}Te chemical shifts for 5 and 6 in CDCl₃ move 78 ppm upfield from Cl to Br as expected in terms of increasing shielding of the tellurium atom.

3 Crystal structure of carbonyl functionalized organotellurium(IV) derivatives 1, 4 and 5

Crystal data and structure refinement details for compounds 1, 4 and 5 are given in Table S1.† ORTEP_s diagrams of 1, 4 and 5 are shown in Fig. 1, 2 and 3 respectively, each captioned with the selected interatomic distances and angles. Table S1† and packing diagrams of 1, 4 and 5 are presented in the ESI (Fig. S1–S10).† Compounds 1 and 4 crystallize in a monoclinic crystal system with the $P2_1/c$ space group, while 5 crystallizes in a monoclinic system with the $P2_1$ space group. The primary geometry around the Te(IV) atom in these diorganotellurium dichlorides is ψ -trigonal bipyramidal with one equatorial position occupied by a stereochemically active lone pair. Interatomic Te \cdots O(carbonyl) distances ($d(\text{Te}\cdots\text{O})$) 2.861(1) Å in

1, 2.847(1) in 4 and 2.926(3) in 5) are longer than the Σr_{cov} (Te,O) of 2.03 Å, and significantly shorter than Σr_{vdw} (Te,O) of 3.58 Å, enough to imply the presence of attractive intramolecular 1,4-Te \cdots O secondary bonding interactions.²⁵ Moreover, the smaller Te–C–C(carbonyl) angle ($104.66(9)^\circ$ in 1, $105.37(9)^\circ$ in 4 and $104.29(16)^\circ$ in 5) compared to the tetrahedral angle indicate appreciable bending, consequentially Te(IV) and O atoms are attracted closer to each other. There are possible rotations about the Te–CH₂ bonds, with the acetylaceton/benzoylaceton fragments in each case being oriented so that the carbonyl oxygen atoms are almost in the equatorial C–Te–C plane. Along with planarity, adjacent linearity of the C(*trans*)–Te \cdots O triad(s) ($155.05(5)^\circ$ 1, $158.51(5)^\circ$ in 4 and $156.82(8)^\circ$ in 5) make $n \rightarrow \sigma^*$ orbital interactions feasible. The observed intramolecular hydrogen bonding interaction in compound 5 (1.744(3) Å) is shorter than compounds 1 (1.824(28) Å) and 4 (1.854(25) Å), probably due to presence of an electron-donating methyl group on the hydroxyl carbon atom. The outstanding feature in all cases is a very short intramolecular O2–H \cdots O1 hydrogen bond [$d(\text{O}\cdots\text{O})$ in the range 2.498(4)–2.559(2) Å]. The downfield shifts of the $\delta(\text{O–H})$ and $\delta(\text{C–H})$ NMR signals are spectroscopic evidences of such strength. In the crystal structures the OH proton is observed to occupy a slightly asymmetric position, supporting all known solid state and solution spectroscopic data.²⁶ Due to the presence of short strong intramolecular hydrogen bonding interactions, C=O and C=C bonds in the adopted six membered rings, together with the carbonyl oxygen and hydroxyl atoms, almost lie in a plane.



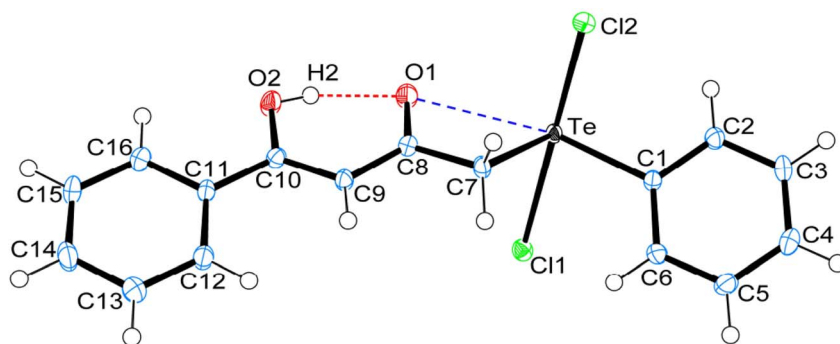


Fig. 1 ORTEPs diagram showing 50% probability displacement ellipsoids and crystallographic numbering scheme for **1**. Selected bond distances (Å) and angles (°): Te–C1 2.126(2), Te–C7 2.137(2), Te–Cl1 2.555(1), Te–Cl2 2.463(1), C8–O1 1.258(2), C10–O2 1.328(2), Te⋯O1, 2.861(1), O1⋯H2, 1.824(28), O2–H2, 0.783(29), O1⋯O2 2.559(2); C1–Te–C7 100.77(6), Te–C7–C8 104.66(9), Cl1–Te–Cl2 171.80(2), Te⋯O1⋯H2 165.45(85), O1⋯H2–O2 153.56(27), C7–Te⋯O1 54.34(4), C1–Te⋯O1 155.05(5), C10–O2⋯H2 104.46(2).

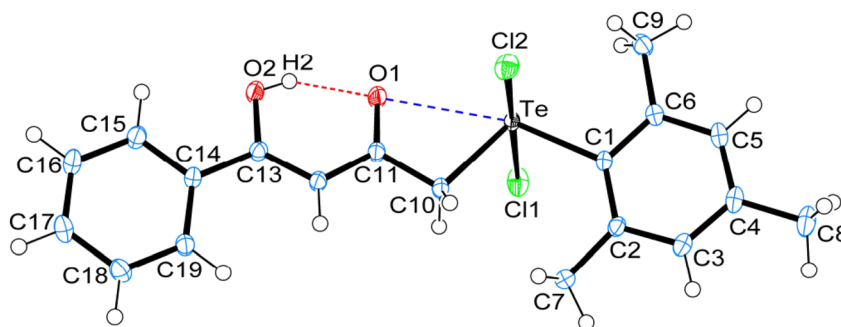


Fig. 2 ORTEPs diagram showing 50% probability displacement ellipsoids and crystallographic numbering scheme for **4**. Selected bond distances (Å) and angles (°): Te–C1 2.125(1), Te–C10 2.148(1), Te–Cl1 2.521(1), Te–Cl2 2.498(1), C11–O1 1.254(2), C13–O2 1.335(2), Te⋯O1, 2.847(1), O1⋯H2, 1.854(25), O2–H2, 0.756(25), O1⋯O2 2.541(2); C1–Te–C10 106.89(54), Te–C10–C11 105.37(9), Cl1–Te–Cl2 173.71(8), Te⋯O1⋯H2 174.65(78), O1⋯H2–O2 159.92(26), C10–Te⋯O1 54.62(4), C1–Te⋯O1 158.51(5), C13–O2⋯H2 107.92(2).

3.1 Supramolecular architectures in the crystal lattices of compound **1**, **4** and **5**

In addition to the short strong intramolecular hydrogen bonding interactions (O⋯H) and Te⋯O secondary bonding interactions, the other intermolecular hydrogen bonding

interactions (C–H⋯O, C–H⋯Cl) and secondary bonding interactions Te⋯Cl and π ⋯ π that have been recognized to play a vital role in the self-assembly of carbonyl functionalized organotellurium(IV) dichlorides. Parametric details of such interactions are depicted in Table S2.†

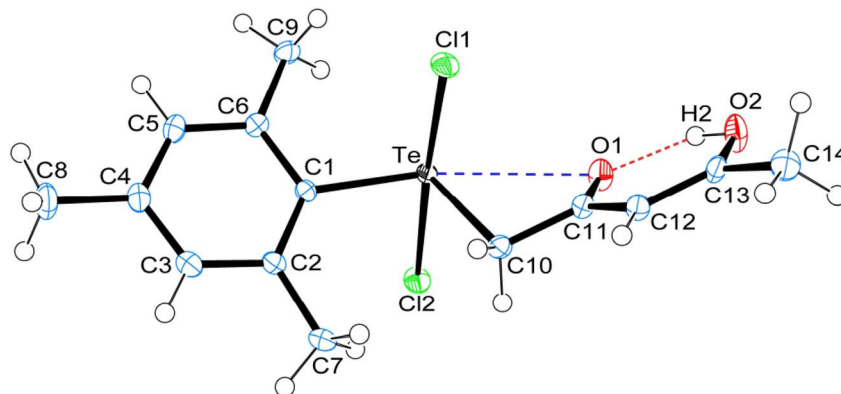


Fig. 3 ORTEPs diagram showing 50% probability displacement ellipsoids and crystallographic numbering scheme for **5**. Selected bond distances (Å) and angles (°): Te–C1 2.127(3), Te–C10 2.141(3), Te–Cl1 2.534(2), Te–Cl2 2.479(2), C11–O1 1.262(3), C13–O2 1.321(3), Te⋯O1, 2.926(3), O1⋯H2, 1.744(3), O2–H2, 0.840(3), O1⋯O2 2.498(4); C1–Te–C10 105.24(10), Te–C10–C11 104.29(16), Cl1–Te–Cl2 173.66(3), Te⋯O1⋯H2 153.18(12), O1⋯H2–O2 148.42(19), C10–Te⋯O1 52.97(8), C1–Te⋯O1 156.82(8), C13–O2⋯H2 109.44(2).



The structure of **1** consists of a 2D helical structure running along the *b*-axis (Fig. S1†), with C–H···Cl interactions along the *c*-axis. Each Te(IV) atom is covalently bonded with two axial Cl atoms and two equatorial C-atoms. Simultaneously each Te(IV) atom is also interconnected with two SBIs [Te···O 2.861(1) Å and Te···Cl 3.477(1) Å] (Fig. S2†). The phenyl ring of benzoylacetone fragment within each helical structure in **1** is glide such that the *para*-carbon atom of one molecule forms a $\pi\cdots\pi$ stacking interaction with the phenyl ring of benzoylacetone fragment of a neighbouring molecule. The *para*-carbon···centroid distance between the phenyl ring of a neighbouring molecule in the structure of **1** is 3.652(2) Å (Fig. S3†). The crystal packing of **1** also consists of a centrosymmetric dimeric unit through C–H···Cl [2.861(1) Å] interactions repetition of these units gives rise to three-dimensional supramolecular architectures *via* self-assembly (Fig. S4†).^{27,28} The crystal structure of **4** consist of a centrosymmetric dimeric unit through reciprocal O–H···O [2.419(24) Å] intermolecular hydrogen bonding interaction (Fig. S5†). These dimeric units further connected with another dimeric unit through reciprocal C–H···Cl [2.902(0) Å] intermolecular hydrogen bonding interaction give rise to a 2D supramolecular architecture along *c*-axis (Fig. S6†). In the dimeric unit of **4** also consist of two strong intramolecular hydrogen bonding interaction C9–H9B···Cl2 [2.881(0) Å] and C7–H7B···Cl1 [2.956(0) Å]. Probably due to these interactions and steric effect of mesityl ring in compound **4** exhibits separate signals for both *ortho* methyl proton (2.74 & 2.79 ppm) and for both *meta* proton (6.43 & 6.97 ppm).

The crystal structure of **5** is devoid of Te based intermolecular SBIs. Steric demand of the mesityl group, acetylacetone fragment and small inter-atomic distance between Te and the axial Cl ligands make the Te atom inaccessible for intermolecular bonding. As a result, chlorine atoms are interconnected through the bifurcated and trifurcated C–H···Cl interactions, along with trifurcated C–H···O inter- and intra-connected hydrogen bonding interaction, giving rise to three-dimensional supramolecular packing (Fig. S7–S9†). Among all three Te(IV) dichlorides, the observed (O–H···O, ~1.95 Å; C–H···O, ~2.47 Å; C–H···Cl, ~2.80 Å and Te···Cl, 3.45 Å) hydrogen bonding and SBIs are longer than Σr_{cov} [(H,O), 0.97 Å; (H,Cl), 1.33 Å; (Te,Cl), 2.40 Å] and significantly shorter than $[\Sigma r_{\text{vdw}}$ (H,O), 2.48 Å; (H,Cl), 2.81 Å; (Te,Cl), 3.83 Å] respectively.²⁵ Linearity of the C–H···O and C–H···Cl make $n \rightarrow \sigma^*$ orbital interaction possible. The four electron-three centre covalent bonding interaction and SBIs play a major role in the formation of supramolecular synthons.

4 Experimental

4.1 General

Preparative work was performed under dry nitrogen. Phenyl, *p*-tolyl, 1-naphthyl, and mesityl tellurium trichlorides were prepared by chlorination of their corresponding ditellurides. Commercial acetylacetone and benzoylacetone were dried with anhydrous Na₂SO₄ and freshly distilled under inert atmosphere. Melting points were recorded in capillary tubes and are uncorrected. The ¹H, ¹³C{¹H}, and ¹²⁵Te NMR spectra were recorded

on Bruker AMX 400, JEOL 400 or JEOL 300 spectrometers. Chemical shifts cited were referenced to TMS (¹H, ¹³C{¹H}) as internal and Me₂Te (¹²⁵Te) as external standard. Microanalyses were carried out using a Carlo Erba 1108 elemental analyzer. Tellurium was estimated volumetrically.

4.2 Syntheses

4.2.1 Reactions of acetylacetone/benzoylacetone with ArTeCl₃ (Ar = Ph, *p*-tolyl, 1-naphthyl, and mesityl). (1) A mixture of phenyltellurium trichloride (0.62 g, 2.0 mmol) and benzoylacetone (0.34 g, 2.1 mmol) was stirred slowly at ~60 °C under a flow of dry nitrogen (~10 h). The resulting paste was washed with cold petroleum ether (3 × 10 mL), triturated with diethyl ether and filtered to remove excess ketone. The residue was dissolved in dichloromethane (25 mL) and filtered through a short silica column. Concentration of the extract to about one third of its original volume and addition of diethyl ether (10 mL) afforded a pale orange solid which was recrystallized from benzene to give **1** as colourless needle shaped crystals. Yield: (0.18 g, 21%); mp 127 °C (from C₆H₆). (Found: C, 44.1; H, 3.3; Te, 29.2. C₁₆H₁₄Cl₂O₂Te requires C, 44.0; H, 3.2; Te, 29.2%); δ_{H} (300.1 MHz; CDCl₃; Me₄Si) 4.78 (2H, s, CH₂), 6.34 (1H, s, CH), 7.44–7.50 (2H, m, aryl), 7.55–7.61 (4H, m, aryl), 7.87–7.89 (2H, m, aryl), 8.21–8.27 (2H, m, aryl), 15.31 (1H, br, OH); δ_{C} (100.5 MHz; CDCl₃; Me₄Si) 62.26 (CH₂), 96.53 (CH), 127.26, 128.80, 130.05, 131.85, 133.05, 133.19, 133.71 (C-Ph), 181.67 (COH), 188.02 (CO); δ_{Te} (126.2 MHz; CDCl₃; Me₂Te) 860.3 (s).

(2) Prepared from *p*-tolyltellurium trichloride (0.65 g, 2.0 mmol) and benzoylacetone (0.34 g, 2.1 mmol) in a way similar to **1**. Yield (0.34 g, 38%); mp 128 °C (from C₆H₆). (Found: C, 45.2; H, 3.6; Te, 28.1. C₁₇H₁₆Cl₂O₂Te requires C, 45.3; H, 3.6; Te, 28.3%); δ_{H} (300.1 MHz; CDCl₃; Me₄Si) 2.44 (3H, s, Me), 4.76 (2H, s, CH₂), 6.34 (1H, s, CH), 7.38 (2H, d, *J* 2.7 Hz, aryl), 7.41–7.50 (2H, m, aryl), 7.55–7.60 (1H, m, aryl), 7.87–7.91 (2H, m, aryl), 8.08–8.14 (2H, m, aryl), 15.31 (1H, br, OH); δ_{C} (100.5 MHz; CDCl₃; Me₄Si) 21.34 (Me), 61.85 (CH₂), 96.61 (CH), 126.42, 127.24, 128.77, 130.78, 133.11, 133.14, 133.53, 142.66 (C-Ph), 181.70 (COH), 187.96 (CO); δ_{Te} (126.2 MHz; CDCl₃; Me₂Te) 863.8 (s).

(3) Prepared from 1-naphthyltellurium trichloride (0.72 g, 2.0 mmol) and benzoylacetone (0.34 g, 2.1 mmol) in a way similar to **1**. Yield (0.81 g, 83%); mp 145 °C (from C₆H₆). (Found: C, 49.3; H, 3.4; Te, 26.1. C₂₀H₁₆Cl₂O₂Te requires C, 49.3; H, 3.3; Te, 26.2%); δ_{H} (300.1 MHz; CDCl₃; Me₄Si) 5.10 (2H, s, CH₂), 6.46 (1H, s, CH), 7.49 (2H, t, *J* 1.9 Hz, aryl), 7.57–7.62 (1H, m, aryl), 7.66 (2H, t, *J* 1.9 Hz, aryl), 7.73 (1H, t, *J* 1.9 Hz, aryl), 7.93 (2H, d, *J* 2.0 Hz, aryl), 7.97 (1H, d, *J* 2.0 Hz, aryl), 8.08 (1H, d, *J* 2.1 Hz, aryl), 8.15 (1H, d, *J* 2.1 Hz, aryl), 8.21 (1H, d, *J* 1.8 Hz, aryl), 15.32 (1H, br, OH); δ_{C} (100.5 MHz; CDCl₃; Me₄Si) 62.57 (CH₂), 96.23 (CH), 126.37, 126.70, 127.25, 128.17, 128.79, 130.70, 132.22, 132.69, 132.77, 133.23, 133.93, 134.22 (C-aryl), 181.05 (COH), 189.08 (CO); δ_{Te} (126.2 MHz; CDCl₃; Me₂Te) 779.5 (s).

(4) Prepared from mesityltellurium trichloride (0.72 g, 2.0 mmol) and benzoylacetone (0.34 g, 2.1 mmol) in a way similar to **1**. Yield (0.33 g, 35%); mp 148 °C (from C₆H₆). (Found: C, 47.7; H, 4.3; Te, 26.7. C₁₉H₂₀Cl₂O₂Te requires C, 47.7; H, 4.2; Te,



26.6%); δ_{H} (300.1 MHz; CDCl_3 ; Me_4Si) 2.32 (3H, s, *p*-Me), 2.74 (3H, s, *o*-Me), 2.79 (3H, s, *o*-Me), 5.09 (2H, s, CH_2), 6.43 (1H, s, CH), 6.97 (1H, s, aryl), 6.99 (1H, s, aryl), 7.48 (2H, t, *J* 1.9 Hz, aryl), 7.58 (1H, t, *J* 1.9 Hz, aryl), 7.91 (2H, d, *J* 1.9 Hz, aryl), 15.34 (1H, br, OH); δ_{C} (100.5 MHz; CDCl_3 ; Me_4Si) 21.01 (*p*-Me), 23.64 (Me), 23.76 (Me), 60.46 (CH_2), 96.48 (CH), 127.30, 128.83, 130.41, 131.59, 133.01, 133.22, 135.47, 139.79, 141.00, 142.34 (C-Mes), 181.38 (COH), 189.40 (CO); δ_{Te} (126.2 MHz; CDCl_3 ; Me_2Te) 802.9 (s).

(5) Prepared from mesityltellurium trichloride (0.72 g, 2.0 mmol) and acetylacetone (1.5 mL, 15 mmol) in a way similar to 1. Yield (0.40 g, 48%); mp 145 °C (from C_6H_6). (Found: C, 40.2; H, 4.6; Te, 30.5. $\text{C}_{14}\text{H}_{18}\text{Cl}_2\text{O}_2\text{Te}$ requires C, 40.3; H, 4.4; Te, 30.6%); δ_{H} (300.1 MHz; CDCl_3 ; Me_4Si) 2.14 (3H, s, *p*-Me), 2.32 (3H, s, Me), 2.70 (3H, s, *o*-Me), 2.80 (3H, s, *o*-Me), 4.95 (2H, s, CH_2), 5.76 (1H, s, CH), 6.99 (1H, s, aryl), 7.03 (1H, s, aryl), 14.7 (1H, br, OH); δ_{C} (100.5 MHz; CDCl_3 ; Me_4Si) 21.00 (*p*-Me), 23.50 (*o*-Me), 23.60 (*o*-Me), 23.7 (Me), 60.10 (CH_2), 100.10 (CH), 130.30, 131.50, 135.20, 139.80, 141.00, 142.30 (C-Mes), 188.10 (COH), 188.40 (CO); δ_{Te} (126.2 MHz; CDCl_3 ; Me_2Te) 801.0 (s).

4.2.2 metathetical reactions of 5. Compound 6 was obtained in a good yield when 5 (0.42 g, 1.0 mmol) and NaBr (0.21 g, 2.0 mmol) were stirred together in chloroform (15 mL) for ~3 h. Sodium bromide was removed by filtration. Addition of petroleum ether (5 mL) and cooling to 0 °C afforded yellow crystals of 6. Yield (0.48 g, 95%); mp 120 °C (from C_6H_6). (Found: C, 33.3; H, 3.6; Te, 25.3. $\text{C}_{14}\text{H}_{18}\text{Br}_2\text{O}_2\text{Te}$ requires C, 33.2; H, 3.6; Te, 25.2%); δ_{H} (300.1 MHz; CDCl_3 ; Me_4Si) 2.14 (3H, s, Me), 2.32 (3H, s, *p*-Me), 2.66 (3H, s, *o*-Me), 2.76 (3H, s, *o*-Me), 5.10 (2H, s, CH_2), 5.76 (1H, s, CH), 6.96 (1H, s, aryl), 7.02 (1H, s, aryl), 14.7 (1H, br, OH); δ_{C} (100.5 MHz; CDCl_3 ; Me_4Si) 20.97 (*p*-Me), 23.36 (*o*-Me), 23.40 (*o*-Me), 24.24 (Me), 59.02 (CH_2), 99.92 (CH), 130.45, 131.58, 131.87, 139.39, 141.12, 142.27 (C-Mes), 187.69 (COH), 188.83 (CO); δ_{Te} (126.2 MHz; CDCl_3 ; Me_2Te) 722.8 (s).

4.2.3 Attempted reductions of 1–5. Individual solutions of 1–5 (1.0 mmol) in dichloromethane (~50 mL) were shaken with an aqueous solution of $\text{Na}_2\text{S}_2\text{O}_5$ (0.19 g, 1.0 mmol) for 10 min. The organic layer gradually turned yellow it was separated and washed with water (4 × 50 mL). The organic fraction was dried over anhydrous Na_2SO_4 and filtered. Volatiles were removed under reduced pressure to give the respective diarylditellurides, Ar_2Te_2 as orange coloured solids, instead of the expected alkylaryltellurides.

4.3. Crystallography

Single crystals of 1, 4 and 5 suitable for X-ray crystallography were grown by slow evaporation of their C_6H_6 solutions at room temperature. ORTEPs and packing diagrams were generated with Ortep 3 for windows²⁹ and DIAMOND 3.2 program respectively.³⁰ Intensity data were collected on a Bruker SMART Apex CCD diffractometer at 100(2) K with graphite-monochromated Mo-K α (0.7107 Å) radiation. The data was integrated with SAINT software.³¹ An experimental absorption modification was applied to the collected reflections with SADABS.³² The structure was confirmed by direct methods using

SHELXTL and was refined on F2 by the full-matrix least-squares procedure using the program SHELXL-2018.³³ All non-hydrogen atoms were refined with anisotropic displacement parameters. Hydrogen atoms attached to carbon were included in geometrically calculated positions using a riding model and were refined isotropically. Packing diagrams for the molecular structures of 1, 4 and 5 are shown in Fig. S1–S10 of the ESI.† Additionally, the ^1H , $^{13}\text{C}\{^1\text{H}\}$ and ^{125}Te NMR spectra are also included in the ESI (Fig. S11–S38).†

5 Conclusions

Electrophilic substitution reaction of aryltellurium trichlorides, ArTeCl_3 (Ar = C_6H_5 , Ph; 4-Me- C_6H_4 , *p*-Tol; 1- C_{10}H_7 , 1-Nap; 2,4,6-Me $_3\text{C}_6\text{H}_2$, Mes) with acetylacetone/benzoylacetone to give carbonyl functionalized unsymmetrical diorganotellurium(IV) dichlorides, Ph[PhC(OH)CHC(O)CH $_2$] TeCl_2 (1), *p*-Tol[PhC(OH)CHC(O)CH $_2$] TeCl_2 (2), 1-Nap[PhC(OH)CHC(O)CH $_2$] TeCl_2 (3), Mes[PhC(OH)CHC(O)CH $_2$] TeCl_2 (4) and Mes[MeC(OH)CHC(O)CH $_2$] TeCl_2 (5). Mes[PhC(OH)CHC(O)CH $_2$] TeBr_2 (6) can also be obtained with 95% yield from the corresponding dichlorides by metathesis with NaBr in chloroform at room temperature. Biphasic ($\text{H}_2\text{O}/\text{CH}_2\text{Cl}_2$) reduction of all the dichlorides with $\text{Na}_2\text{S}_2\text{O}_5$ affords labile tellurides, which decompose quickly even at room temperature into the more stable symmetric ditellurides, Ar_2Te_2 . Mesityl fragments bearing organotellurium(IV) derivatives show separate ^1H and $^{13}\text{C}\{^1\text{H}\}$ NMR signals for the *ortho* methyls and meta protons of the mesityl ring.

Data availability

The data supporting this article have been included as part of the ESI.† Crystallographic data for compounds 1, 4 & 5 has been deposited at the Cambridge Crystallographic Data Centre (CCDC) under accession numbers 2378222, 2378223 and 2378224 and can be obtained from “<https://www.ccdc.cam.ac.uk/>”.

Conflicts of interest

There are no conflicts of interest to declare.

Acknowledgements

PS is heartily thankful to the Science and Engineering Research Board, New Delhi, India, for Teachers Associateship for Research Excellence Grant (Project No. TAR/2021/000075). MK and PS are particularly grateful to Dr R. C. Srivastava and Dr Ashok Kumar Singh Chauhan (Retired Professor of Department of Chemistry, University of Lucknow) for guidance and valuable suggestions. We are also thankful to Central Drug Research Institute Lucknow for recording analytical data.

References

- G. S. Hammond, W. G. Borduin and G. A. Guter, *J. Am. Chem. Soc.*, 1959, **81**, 4682–4686.



- 2 M. S. Gordon and R. D. Koob, *J. Am. Chem. Soc.*, 1973, **95**, 5863–5867.
- 3 R. H. Holm and F. A. Cotton, *J. Am. Chem. Soc.*, 1958, **80**, 5658–5663.
- 4 B. Bock, K. Flatau, H. Junge, M. Kuhr and H. Musso, *Angew. Chem., Int. Ed. Engl.*, 1971, **10**, 225–235.
- 5 X.-B. Chen, W.-H. Fang and D. L. Phillips, *J. Phys. Chem. A*, 2006, **110**, 4434–4441.
- 6 B. Schiütt, B. B. Iversen, G. K. H. Madsen and T. C. Bruice, *J. Am. Chem. Soc.*, 1998, **120**, 12117–12124.
- 7 H. Matsuzawa, T. Nakagaki and M. Iwahashi, *J. Oleo Sci.*, 2007, **56**, 653–658.
- 8 G. A. Jeffrey and W. Saenger, *Hydrogen Bonding in Biological Structures*, Springer, Berlin, 1991.
- 9 (a) C. B. Aakeroy, *Acta Crystallogr.*, 1997, **B53**, 569–586; (b) G. R. Desiraju, *Chem. Commun.*, 1997, 1475–1482.
- 10 (a) P. Y. Feng, X. H. Bu and G. D. Stucky, *Nature*, 1997, **388**, 735–741; (b) X. H. Bu, P. Y. Feng and G. D. Stucky, *Science*, 1997, **278**, 2080–2085.
- 11 F. Huang and E. V. Anslyn, *Chem. Rev.*, 2015, **115**, 6999–7000.
- 12 B. J. Eckstein, L. C. Brown, B. C. Noll, M. P. Moghadasnia, G. J. Balaich and C. M. McGuirk, *J. Am. Chem. Soc.*, 2021, **143**, 20207–20215.
- 13 W. Yang, R. Jiang, C. Liu, B. Yu, X. Cai and H. Wang, *Cryst. Growth Des.*, 2021, **21**, 6497–6503.
- 14 E. R. T. Tiekink, *Coord. Chem. Rev.*, 2022, **457**, 214397.
- 15 S. Benz, J. Mareda, C. Besnard, N. Sakai and S. Matile, *Chem. Sci.*, 2017, **8**, 8164–8169.
- 16 S. Benz, J. López-Andarias, J. Mareda, N. Sakai and S. Matile, *Angew. Chem., Int. Ed.*, 2017, **56**, 812–815.
- 17 P. Wönnner, L. Vogel, F. Kniep and S. M. Huber, *Chem.–Eur. J.*, 2017, **23**, 16972–16975.
- 18 P. Pale and V. Mamane, *Chem.–Eur. J.*, 2023, **29**, e202302755.
- 19 L. T. Maltz and F. P. Gabbaï, *Organometallics*, 2024, **43**, 1246–1255.
- 20 M. B. Smith and J. March, *Advanced Organic Chemistry Reaction, Mechanism and Structure*, 6th edn, 2013, ch. 2, pp. 99–101.
- 21 (a) G. T. Morgan and H. D. K. Drew, *J. Chem. Soc.*, 1920, **117**, 1456–1465; (b) G. T. Morgan and H. D. K. Drew, *J. Chem. Soc.*, 1921, **119**, 610–625; (c) G. T. Morgan and H. D. K. Drew, *J. Chem. Soc.*, 1922, **121**, 922–940; (d) G. T. Morgan and H. G. Reeve, *J. Chem. Soc., Trans.*, 1923, **123**, 444–452; (e) G. T. Morgan and H. D. K. Drew, *J. Chem. Soc.*, 1924, **125**, 731–754; (f) G. T. Morgan and R. W. Thomason, *J. Chem. Soc., Trans.*, 1924, **125**, 754–759; (g) G. T. Morgan and E. Holmes, *J. Chem. Soc., Trans.*, 1924, **125**, 760–765; (h) G. T. Morgan and C. R. Porter, *J. Chem. Soc.*, 1924, **125**, 1269–1277; (i) G. T. Morgan and H. D. K. Drew, *J. Chem. Soc.*, 1924, **125**, 1601–1607; (j) G. T. Morgan and H. D. K. Drew, *J. Chem. Soc.*, 1925, **127**, 531–538; (k) G. T. Morgan, F. J. Corby, O. C. Elvins, E. Jones, R. E. Kellert and C. J. A. Taylor, *J. Chem. Soc.*, 1925, **127**, 2611–2625; (l) D. H. Dewar, J. E. Fergusson, P. R. Hentschel, C. J. Wilkins and P. P. William, *J. Chem. Soc.*, 1964, 688–691.
- 22 Y. Kawasaki and R. Okawara, *Bull. Chem. Soc. Jpn.*, 1967, **40**, 428.
- 23 (a) A. K. S. Chauhan, P. Singh, A. Kumar, R. C. Srivastava, R. J. Butcher and A. Duthie, *Organometallics*, 2007, **26**, 1955–1959; (b) A. K. S. Chauhan, P. Singh, R. C. Srivastava, A. Duthie and A. Voda, *Dalton Trans.*, 2008, 4023–4028; (c) A. K. S. Chauhan, P. Singh, R. C. Srivastava, R. J. Butcher and A. Duthie, *J. Organomet. Chem.*, 2010, **695**, 2118–2125.
- 24 Y. Takaguchi, H. Fujihara and N. Furukawa, *J. Organomet. Chem.*, 1995, **498**, 49–52.
- 25 (a) O. Niyomura, S. Kato and S. Inagaki, *J. Am. Chem. Soc.*, 2000, **122**, 2132–2133; (b) A. Bondi, *J. Phys. Chem.*, 1964, **68**, 441–451.
- 26 V. Bertolasi, P. Gilli, V. Ferretti and G. Gilli, *J. Am. Chem. Soc.*, 1991, **113**, 4917–4925.
- 27 G. R. Desiraju, *Angew. Chem., Int. Ed. Engl.*, 1995, **34**, 2311–2327.
- 28 D. Braga and F. Grepioni, *Acc. Chem. Res.*, 2000, **33**, 601–608.
- 29 L. J. Farrugia, *J. Appl. Crystallogr.*, 2012, **45**, 849–854.
- 30 K. Brandenburg and H. Putz, *DIAMOND (v. 3.2e)*, *Crystal Impact GbR*, 1997–2012.
- 31 Bruker, *SAINT*, Bruker AXS Inc., Madison, 2016.
- 32 SADABS, *Area Detector Absorption Correction Program*, Bruker Analytical X-ray, Madison, 2018.
- 33 G. M. Sheldrick, *Acta Crystallogr.*, 2015, **C71**, 1–3.

